Polish Society of Composite Materials
Polskie Towarzystwo Materiałów Kompozytowych

19: 4 (2019) 161-168

COMPOSITES THEORY AND PRACTICE
ISSN: 2084-6096
ISSN (online): 2299-128X

Michał Stawiarz[1], Paweł Kurtyka[2]*, Natalia Rylko[2], Simon Gluzman[3]

[1]Independent Researcher in collaboration with Materialica + Research Group, Poland
[2]Institute of Technology, Pedagogical University of Krakow, ul. Podchorążych 2, 30-084 Krakow, Materialica + Research Group, Poland
[3]Independent Researcher in collaboration with Materialica + Research Group, 606-3000 Bathurst St., Toronto, ON, M6B 3B4, Canada
**Corresponding author: E-mail: pkurtyka@up.krakow.pl*

Received (Otrzymano) 8.12.2019

INFLUENCE OF FSP PROCESS MODIFICATION ON SELECTED PROPERTIES OF Al-Si-Cu/SiC$_p$ COMPOSITE SURFACE LAYER

The paper presents the results of mechanical and tribological tests conducted on the surface of Al-Si-Cu/SiC$_p$ composite reinforced with SiC particles and modified by friction stir processing (FSP) with different parameters. Changes in the distribution of the reinforcement particles on the modified surface of the composite were calculated and analyzed using a new analytical RVE theory with Eisenstein-Rayleigh-Mityushev sums (ERM-sum) (see the definitions below), and PointSel software. The Vickers hardness test with a 1 N load and the ball-on-disc method were used to test the material properties. A high degree of homogenization of the tested material was observed as a result of its modification, as evidenced by an approximately 4-fold reduction in the size of representative volume element (RVE) cells. The size of the RVE cell decreased almost four times for the material after modification, which indicates the high level of homogenization of the tested material. Moreover, we observed a reduction by order of magnitude of the anisotropy coefficient of the distribution of the reinforcing phase particles after the modification process. A 30% increase in the Vickers microhardness of the representative areas was obtained for the modified composites. After the FSP modification process the friction coefficient increases by 40%, and almost 25% decrease in the specific wear rate is observed. Both effects are attributed to the achieved homogenization of particle distribution and reduction of particle size up to 38%.

Keywords: aluminium matrix composite, structure analysis, mechanical properties, tribological behaviour, ball-on-disc method

WPŁYW MODYFIKACJI PROCESU FSP NA WYBRANE WŁAŚCIWOŚCI WARSTWY WIERZCHNIEJ W KOMPOZYTACH Al-Si-Cu/SiC$_p$

Przedstawiono wyniki badań właściwości mechanicznych i tribologicznych powierzchni kompozytów Al-Si-Cu/SiC$_p$ modyfikowanych metodą FSP z różnymi parametrami. Zmianę rozkładu cząstek wzmacniających na powierzchni kompozytu zbadano z wykorzystaniem nowej analitycznej teorii RVE oraz ERM-sums i programu PointSel. Testy twardości przeprowadzono metodą Vickersa przy obciążeniu 1 N, a testy ścieralności wykonano metodą ball-on-disc. Po procesie modyfikacji stwierdzono wysoki stopień homogenizacji, który cechował się około czterokrotnym zmniejszeniem wielkości komórki RVEc oraz spadkiem o rząd wielkości wartości współczynnika anizotropii rozkładu cząstek fazy wzmacniającej. Zaobserwowano około 30% wzrost mikrotwardości Vickersa w modyfikowanym kompozycie. Po procesie modyfikacji FSP stwierdzono również 40% wzrost wartości współczynnika tarcia oraz blisko 25% spadek wartości wskaźnika zużycia, wynikający z ujednorodnienia struktury i redukcji wielkości cząstek SiC, dochodzącej do 38%.

Słowa kluczowe: kompozyt z osnową aluminiową, analiza struktury, właściwości mechaniczne, zachowanie tribologiczne, metoda ball-on-disc

INTRODUCTION

In recent years, increased interest has been observed in novel composite materials, in particular based on aluminium alloys. Currently, these materials successfully replace conventional steels and aluminium alloys in the automotive, aerospace and shipbuilding industry, mainly due to their mechanical properties superior to conventional materials and/or increased resistance to tribological wear with the same or even reduced material density [1].

Parallel to studies of the properties of new composite materials, intensive research is being carried out on the methods of their fabrication [2-6], joining [7, 8], or modification [9, 10] to optimize technology and reduce costs [11, 12].

Numerous factors affect the properties of composite materials, including the selected manufacturing technology and technological process parameters. However, the main factor determining the macroscopic properties of the composite is the choice of the reinforcing phase: its properties, volume fraction [13, 14] and geometrical parameters of the reinforcing phase distribution [15-19].

As for the mechanical and tribological properties, any increase in volume fraction of the reinforcing phase leads to their improvement. The relationship between the hardness and reinforcement content is almost linear. Nonlinear dependencies appear at high volume fractions, closer to the percolation threshold for the reinforcing phase [20]. For composites based on aluminium alloys reinforced with SiC, Al_2O_3 or TiC particles, improvement can reach 140% of the value measured for a pure matrix at room temperatures [21, 22]. It should be noted that the described trend also occurs at high temperatures, although to a lesser extent [23]. As was mentioned above, increasing the proportional fraction of the reinforcing phase also improves the tribological properties of composites. Consequently, doubling the content of the reinforcing phase increases the resistance to abrasion (reduced weight loss) by 70% [21, 24]. Another factor responsible for the mechanical and tribological properties of composites is the average size of the particles in the reinforcing phase [13, 14]. As an example, one can consider the results of hardness tests carried out on composites reinforced with SiC or Al_2O_3 particles in the size range varying from 23 to 478 μm [22, 23]. The obtained results indicate an almost linear decrease in hardness with an increasing particle size, amounting to about 30% decrease at room temperatures and to a 15% decrease at elevated temperatures. The influence of the size of reinforcing particles on the tribological properties is no longer as unambiguous as in the case of hardness. For example, in [25] it is reported that for Al_2O_3 particles with sizes in the range of 25÷50 μm, the wear rate increases, while it decreases in the range of 10÷25 μm.

The size of the particles of the reinforcing phase also affects composite fracture/cracking during its usage. In [26-28] it was found that reducing the particle size reduces the density of cracks resulting from mechanical loading. This in turn, reduces the density of the fragments of reinforcement "knocked out" of the matrix as a result of friction wear. This phenomenon was described in [25], where the authors investigated the effect of the size of Al_2O_3 particles on the wear rate. The authors noticed that when the particle size exceeded 50 μm, the process of breaking and release of the fragments of particles occurred as a result of friction wear, and the broken and released fragments were deposited in the contact layers, resulting in increased wear of the material. Knowledge about the impact of the geometrical parameters of the reinforcing phase on the mechanical and tribological properties of composites as well as the observation of particle behavior under loading have prompted the researchers to look for new technological solutions to allow further optimization of composite structures in the process of their production and modification. Increasingly, methods based on severe plastic deformation (SPD) are used for this purpose, including friction stir processing technologies (FSP) [29], allowing the manufacturing [30, 31], modification [32, 33] and joining of composite materials [34] without any adverse effect on and even with some improvement of their mechanical and tribological properties [35-37].

The above facts have served as an inspiration to investigate the influence of the FSP process parameters on Al-Si-Cu/SiC_p composite modification in terms of changes in selected mechanical and tribological properties and also in the geometrical parameters of the reinforcement distribution in representative RVE cells.

All of the above have served as an inspiration to investigate the influence of the FSP process parameters on Al-Si-Cu/SiC_p composite modification in terms of changes in selected mechanical and tribological properties and also in the geometrical parameters of the reinforcement distribution in RVE cells. The RVE (representative volume element) is constructed for experimental concentration of the particles of the reinforcing SiC phase. Rigorous definition of RVE involving ERM-sums is mainly due to Mityushev, and can be found in [38].

Intuitively, RVE corresponds to a minimal sized sample that is structurally entirely typical of the whole composite on average, and contains a sufficient number of inclusions for the apparent mechanical properties to be effectively independent of the boundary values of traction and displacement.

In the case under discussion, the RVE cell is built by exploring the concentration of the particles of the reinforcing phase. Determining the RVE cell starts with measuring the concentration in a randomly selected 2D section of the composite.

It is assumed that the analyzed region will always have a square shape. Assigning the particles to a given cell is based on the determination of their center and checking whether it was inside the designated region. Calculations were carried out for regions containing from N_{min}(= 10) to N_{max}(= 5000) particles with a calculation increment of δN(= 10) particles. The essence of the method consists in building a cell with a certain concentration of reinforcing particles, specifying the number of particles in this cell, and calculating the concentration of the reinforcing phase. In the next iteration, the number of particles was raised by 10, and then the concentration to be recalculated for the successively growing regions. The goal is to find the region where concentration stabilization began. The RVE cell is built to contain the number of particles of the reinforcing phase considered as a minimal essential value for concentration stabilization [17].

MATERIALS AND EXPERIMENTAL PROCEDURE

As the test material a cast aluminium alloy matrix composite reinforced with SiC particles with an average size of about 15 μm and concentration of 10% was chosen. The composition of the composite matrix alloy according to the manufacturer data is given in Table 1. Detailed descriptions of the typical microstructure components and matrix properties can be found, among others, in the studies of similar alloys [39-41].

From the cast ingot, 4 mm thick plates with 100 x 100 mm dimensions were cut out. The FSP process was carried out with the conventional tools, in the casting direction at rotational speeds of 560 rpm (variants: 560-1 for single process, 560-2 for double process) and 900 rpm (variants: 900-1 for single process, 900-2 for double process) with linear velocities of 355 mm/min for both speeds. Modification was carried out on the plate surface along the preset lines. A detailed description of the FSW/FSP process is given in [16, 42-45].

TABLE 1. **Chemical composition of Al-Si-Cu/SiC$_p$ composite matrix**
TABELA 1. **Skład chemiczny osnowy kompozytu Al-Si-Cu/SiC$_p$**

Alloy	Content of elements [wt.%]						
	Si	Cu	Ni	Mg	Fe	Ti	Al
AlSiCu	10.5	3.2	1	1	0.25	0.25	Bal.

The microstructure was examined on the surface of the plate under the shoulder on materials in both an unmodified and modified condition using an OLYMPUS GX51 light microscope (LM). A panorama of the sample macrostructure images was created in Microsoft Image Composite Editor (ICE), combining several images obtained by light microscopy. Scanning electron microscopy (SEM) was conducted using a JEOL 6610 LV microscope with an energy-dispersive spectrometer EDS and Aztec Software. The procedure of preparing the surface for examinations included mechanical grinding with abrasive paper of a 240 to 1500 grit size, followed by polishing with Struers discs and diamond pastes of 9 to 1 μm. The samples were not etched. The sample surfaces were assessed for the degree of change in the distribution and concentration of the reinforcing SiC particles using calculations based on RVE theory [46] and a new structure assessment method proposed by Rylko and Kurtyka [17], which applies a non-standard advanced matrix calculation and Eisenstein-Rayleigh-Mityushev sums (ERM-sum) [47, 48]. Analysis based on RVE theory was conducted in a Wolfram Mathematica 11 package.

The mechanical properties of the composite in both the unmodified and modified condition were determined by the Vickers microhardness test on an Innovatest 4003 hardness machine under a load of 1 N. The series of microhardness tests consisted of nine measurements, forming a matrix of imprints with dimensions consistent with the size of the RVE cell. The tribological properties were examined by the ball-on-disc method with the following parameters:

- ball - Al_2O_3
- diameter - 1.8 inch
- loads - 4 N
- test time - 10000 s
- rotation speed - 192 rpm

The wear tracks were subjected to profilometry tests using a TOPO 01P contact profilometer with an inductive measuring head with a 2 μm radius tip and 90° cone angle.

RESULTS AND DISCUSSION

Structure

To evaluate the effect of the FSP process in terms of the Al-Si-Cu/SiC$_p$ composite surface modification, structural analysis by LM and SEM was used as well as a new research methodology described in [17], based on RVE and ERM-sum theory [38, 47-49]. The material was examined in the as-cast state and after modification carried out in four variants at various rotational speeds and number of tool passes. Already at the LM observation stage, significant changes in the composite structure were found after modification as compared to the unmodified state (Fig. 1).

a) b)

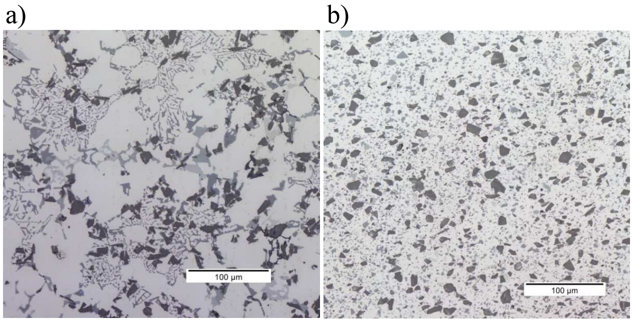

Fig. 1. Microstructure of Al-Si-Cu/SiC$_p$ composite: a) initial state - dendritic structure, nonuniform distribution of reinforcing SiC particles, b) modified (560 rpm) - uniform distribution and decreasing size of reinforcing phase

Rys. 1. Mikrostruktura kompozytu Al-Si-Cu/SiC$_p$: a) stan wyjściowy - struktura dendrytyczna, niejednorodny rozkład cząstek fazy wzmacniającej, b) po modyfikacji (560 rpm) - jednorodny rozkład oraz zmniejszenie rozmiarów cząstek fazy wzmacniającej

Regardless of the parameters used in the FSP process, the structure of the modified material showed a significant degree of fragmentation of the phases, including the SiC reinforcing phase. A more uniform distribution of the reinforcing particles was also observed. To quantify the observed changes a representative volume element RVEc was determined by applying the developed methodology for each of the examined variants. The results are presented in Figure 2. This approach seems to be necessary to correctly assess the effect of the process on the properties of the modified layer, among others, due to large discrepancies in literature reports on this issue [50-52].

Figure 2a clearly shows the beginning of stabilization of the reinforcing phase concentration at the cell containing about 2000 SiC particles, thus specifying the RVE cell size for the material before modification. The same analysis was carried out for the modified composite. Figure 2b indicates a stepwise, almost fourfold decrease in the size of the RVE cell to a level of about 400-500 SiC particles relative to the starting material. A reduction in the RVE cell size after modification of the starting material was observed in all the studied variants, but the fact that the modification parameters had but only a negligible effect on these values deserves particular attention.

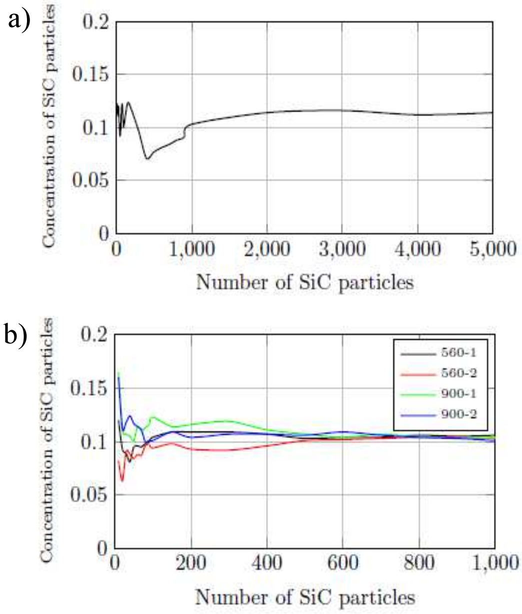

Fig. 2. Changes in concentration of reinforcing phase particles examined in selected square areas with preset number of particles: a) composite in initial state and b) modified

Rys. 2. Zmiany koncentracji fazy wzmacniającej w funkcji wielkości obszaru, określanego ilością cząstek wzmacniających: a) kompozyt w stanie wyjściowym, b) kompozyt w stanie modyfikowanym

The observed changes in the RVE cell size as a result of the FSP process also confirm the positive effect of the process on homogenization of the concentration, thus confirming literature reports [53, 54] and introducing a parametric evaluation of the level of homogenization.

Data about the size of the RVE cells in the material before and after modification enabled calculation of the anisotropy coefficient of the reinforcing phase distribution. Equation (2) was used for this purpose in accordance with the methodology described in [17].

In mathematical modeling, the general definition of ERM-sums $e_{m1...mq}$ is given as follows [38]:

$$e_{m_1...m_q} := N^{-[1+\frac{1}{2}(m_1|+...+m_q)]} \sum_{k_0 k_1 ... k_q} E_{m_1}(a_{k_0} - a_{k_1}) \times \overline{E_{m_2}(a_{k_1} - a_{k2})} ... \mathbf{C}^{q+1} E_{m_q}(a_{k_{q-1}} - a_{k_q}) \quad (1)$$

In practical applications of mathematical definitions, it is sum e_2 which is important. Recently, it has been shown that also some other ERM-sums have transparent geometrical meaning [20]. This is given by Equation (1) and anisotropy factor κ is calculated from this sum as expressed by Equation (2) [47, 48]

$$\kappa = \frac{1}{2\pi N^2} \left| \mathrm{Re} \sum_{k=1}^{N} \left[\sum_{m \neq k}^{N} E_2(a_k - a_m) - \pi \right] \right| \quad (2)$$

Here, a_k denotes the complex coordinate of the center of the kth inclusion and $E_m(z)$ the Eisenstein series, described in [47, 48], the bar denotes the complex conjugation, N the number of inclusions per cell. It is here assumed for convenience that **C** also stands for the operator of complex conjugation and $E_m(0) = S_m$, where S_m denotes the lattice sum of order m. When $\kappa = 0$ the material is isotropic, and the degree of anisotropy increases as κ increases.

The anisotropy coefficients of the reinforcing phase distribution were calculated in the RVE cells for the material before and after modifications. The results are shown in Figure 3. It was observed that anisotropy coefficient κ obtained for the base material was higher than the value obtained for the modified materials by one order of magnitude.

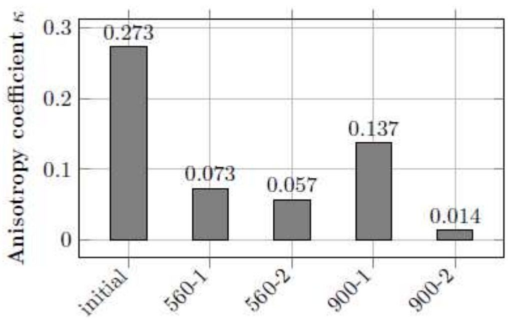

Fig. 3. Changes in anisotropy coefficient for composites Al-Si-Cu/SiC_p in initial state and all modified variants

Rys. 3. Zależność zmian współczynnika anizotropii dla kolejnych wariantów kompozytu Al-Si-Cu/SiC_p

Differences in κ coefficient for the modification variants were observed, caused by the change of the rotational speed of the tool (Fig. 3). For example, a higher degree of homogenization of the reinforcing phase distribution was obtained with a single pass at the speed of 560 rpm, but in the case of a double pass, better homogenization effects were obtained at 900 rpm (Fig. 3). For example, for the speed of 560 rpm, the differences between single and double tool passes were about 30%, while at 900 rpm the difference reached almost 90%.

In addition, image analysis was performed to determine the particle size of the reinforcing phase in the RVEc areas for all the tested variants and the value of the surface share of the reinforcing phase was calculated. The results obtained at the level of 10% are consistent with the data provided by the manufacturer. Checking this parameter after receiving microstructure micrographs is extremely important because of the possibility of errors resulting from poorly selected parameters of image processing analysis [55].

The average value of the size of the reinforcing particles in the material after modification decreased by about 40% for the speed of 560 rpm and about 20% for the speed of 900 rpm, the results obtained for all the tested variants are given in Figure 4. The fragmentation of the reinforcing phase described above occurs as a result of standard, well-known processes accompanying FSP methods [56-59].

The fact that after the second pass, for both tested speeds, the average size of the particles increased by a very small degree only, which should probably be associated with the formation of a significant amount (up to several percent) of particles with sizes at the limit of microscope resolution, deserves some attention. Considered uncertain, these particles were neglected in further analysis.

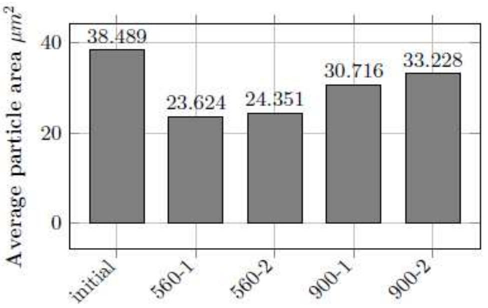

Fig. 4. Average particle size for Al-Si-Cu/SiC$_p$ composites in initial and modified states

Rys. 4. Średnia wielkość cząstek wzmacniających dla kolejnych wariantów kompozytu Al-Si-Cu/SiC$_p$ w stanie wyjściowym i po modyfikacji

Mechanical properties

The results of the microhardness tests for each tested sample are summarized in Table 2. Analysis of the changes in the average value of hardness indicates its increase after modification in the range from 32% to 45% in comparison to the base material. The result is in line with expectations and is also confirmed in [16].

TABLE 2. **Results for Vickers microhardness HV_{01} tests for composite Al-Si-Cu/SiC$_p$ in initial and modified state**

TABELA 2. **Wyniki badania mikrotwadości HV_{01} metodą Vickersa dla kompozytu Al-Si-Cu/SiC$_p$ w stanie wyjściowym i modyfikowanym**

Material	HV_{01min}	HV_{01max}	Average	STD, σ
base	102	200	125	20.564
560-1	160	215	175.3	10.923
560-2	148	200	166.3	10.734
900-1	156	201	177.6	9.134
900-2	147	196	174.8	10.777

Noteworthy is the fact that the differences in the average hardness values are less than 5%. In addition, changes in the average values are the result of a significant shift towards achieving higher minimum values, leaving the maximum at the level of slight differences [16]. A slight decrease in the hardness value at the next pass of the tool can be explained by the processes of structural regeneration occurring during modification [59-62].

Tribological properties

Changes in the structure of the surface layer of the composite after modification also affect the tribological properties of the tested material, which were explored in the ball-on-disc abrasion test. The total test distance was equal to 743 m and the total test time was 10 000 s. For the material in the initial state, the average value of the friction coefficient μ was equal to 0.317, for the composite after modification the average values of the friction coefficient were increased to the level of 0.415 for sample 900-2, and to the level of 0.449 for both samples 560-1 and 560-2. Comparing the friction coefficient plots for the material before and after modification, greater stability of the results for the modified material, with the exception of sample 560-2 can be noticed. Comparing the friction coefficient plots for the material before and after modification, greater stability of the results for the modified material, except sample 560-2 are observed. In this case, the value of the friction coefficient oscillated significantly between 8200 s and 8400 s of the experiment. Probably this phenomena was caused by the occurrence of a large inhomogeneous area on the wear track. We point out that in all the calculations of the averages, we omitted the friction coefficients obtained during the first 2000 s of the test duration (material break-in time).

The average values of the friction coefficient with standard deviations are shown in Figure 5.

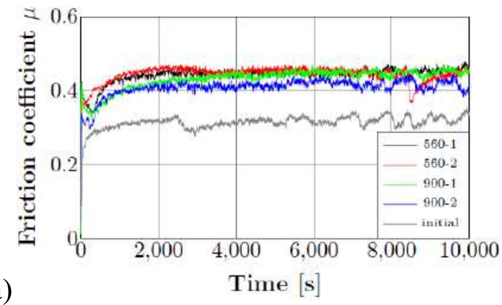

a)

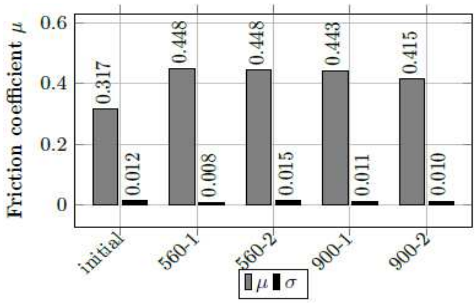

b)

Fig. 5. Typical friction coefficient curves obtained under load of 4 N at sliding speed of 0.1 m/s (a) and average friction coefficient with STD value for Al-Si-Cu/SiC$_p$ composite in initial and modified states (b)

Rys. 5. Typowe krzywe zmian współczynnika tarcia otrzymane pod obciążeniem 4 N z prędkością ścierania 0.1 m/s (a) i średnie wartości współczynnika tarcia wraz z odchyleniem standardowym dla Al-Si-Cu/SiC$_p$ kompozytu w stanie wyjściowym i modyfikowanym (b)

Based on the results of profilometry studies of the wear tracks left by the ball-on-disc test, it was found that the specific wear rate was definitely higher for the base material (327.43 mm^3/Nm) than for other materials (from 244.25 to 251.33 mm^3/Nm). This is mainly due to significant improvement of the SiC phase distribution in the composite after modification. The results of the wear test are compared for all the tested variants in Figure 6.

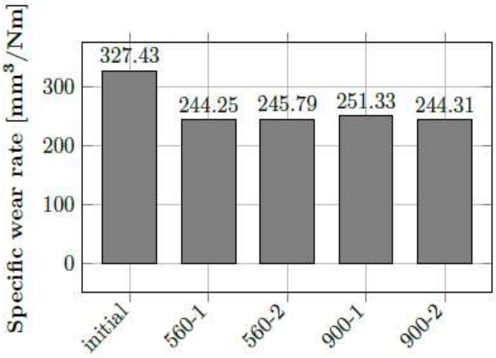

Fig. 6. Values of specific wear rate of Al-Si-Cu/SiC_p composite in initial and modified states tested under load 4 N at sliding speed of 0.1 m/s

Rys. 6. Wartości wskaźnika zużycia dla kompozytu Al-Si-Cu/SiC_p w stanie wyjściowym i modyfikowanego, badanego pod obciążeniem 4 N i prędkością ścierania 0,1 m/s

CONCLUSIONS

Extensive studies were carried out to investigate the impact of the FSP modification parameters on the selected mechanical and tribological properties, as well as the structural parameters of the reinforcing phase in the Al-Si-Cu/SiC_p composite.

Based on the results obtained in the conducted research the following was found:

1. The higher level of homogenization of the tested material is the result of its modification, as evidenced by an approximately 4-fold reduction in the size of RVE cells and a reduction by order of magnitude in the coefficient of anisotropy of the distribution of the reinforcing phase particles.
2. A reduction in the size of the particles of the reinforcing phase reaching its maximum for various rotational speeds of the tool, amounting to 38.5% for the variants of the modified material 560-1 and 13.7% for variant 900-2.
3. An almost 30% increase in the microhardness of the representative areas combined with a high level of homogeneity as evidenced by an almost twofold decrease in the standard deviation obtained for the modified composites.
4. A 40% increase in the coefficient of friction of the modified materials compared to the base material.

Acknowledgements

This work was funded by the Research Fund of the Institute of Technology of the Pedagogical University of Krakow.

One of the authors (P.K) expresses his appreciation to Adam Pietras Dr.Eng. from the Institute of Welding in Gliwice for efforts related to composite modification. Sincere words of gratitude are also extended to Professor Vladimir Mityushev for his valuable advice. The authors would like to thank Paweł Jochym for coding the PointSel software.

REFERENCES

[1] Sharifi E.M., Karimzadeh F., Enayati M., Fabrication and evaluation of mechanical and tribological properties of boron carbide reinforced aluminum matrix nanocomposites, Materials and Design 2011, 32, 6, 3263-3271.

[2] Salehi M., Farnoush H., Mohandesi J.A., Fabrication and characterization of functionally graded alsic nanocomposite by using a novel multistep friction stir processing, Materials and Design 2014, 63, 419-426.

[3] Szymański Ł., Olejnik E., Tokarski T., Kurtyka P., Drożynski D., Żymankowska-Kumon S., Reactive casting coatings for obtaining in situ composite layers based on fe alloys, Surface and Coatings Technology 2018, 350, 346-358.

[4] Dolata A.J., Dyzia M., Jaegermann Z., Structure and physical properties of alumina ceramic foams designed for centrifugal infiltration process, Composites Theory and Practice 2017, 17(3), 136-143.

[5] Olejnik E., Szymański Ł., Tokarski T., Tumidajewicz M., Tic - based local composite reinforcement obtained in situ in ductile iron based castings with use of rode preform, Materials Letters 2018, 222, 192-195.

[6] Boczkal S., Dolata A.J., Nowak M., Effect of SiC and GR reinforcement particles on the structure and functional properties of composite casting, Archives of Metallurgy and Materials 2016, 61, 1, 399-404.

[7] Zhang X., Quan G., Wei W., Preliminary investigation on joining performance of SiC_p-reinforced aluminium metal matrix composite (Al/SiCp-mmc) by vacuum brazing, Composites Part A: Applied Science and Manufacturing 1999, June, 30, 6, 823-827.

[8] Ellis M.B.D., Joining of Al-based metal matrix composites - a review, Materials and Manufacturing Processes 2007, April, 11, 1, 45-66.

[9] Taha M.A., Practicalization of cast metal matrix composites (mmccs), Materials & Design 2001, September, 22, 6, 431--441.

[10] Ibrahim I.A., Mohamed F.A., Lavernia E.J., Particulate reinforced metal matrix composites - a review, Journal of Materials Science 1991, March, 26, 5, 1137-1156.

[11] Miracle D., Metal matrix composites - from science to technological significance, Composites Science and Technology 2005, 65, 15, 2526-2540.

[12] Hashim J., Looney L., Hashmi M., Metal matrix composites: production by the stir casting method, Journal of Materials Processing Technology 1999, August, 92-93, 1-7.

[13] Yueguang W., Particulate size effects in the particle-reinforced metal-matrix composites, Acta Mechanica Sinica 2001, February 17, 1, 45-58.

[14] Zhang P., Li F., Effect of particle characteristics on deformation of particle reinforced metal matrix composites, Transactions of Nonferrous Metals Society of China 2010, 20, 4, 655-661.

[15] Li Y., Ramesh K., Influence of particle volume fraction, shape, and aspect ratio on the behavior of particle-reinforced metal- matrix composites at high rates of strain, Acta Materialia 1998, 46, 16, 5633-5646.

[16] Kurtyka P., Rylko N., Tokarski T., Wójcicka A., Pietras A., Cast aluminium matrix composites modified with using FSP process changing of the structure and mechanical properties, Composite Structures 2015, August, 133, 959-967.

[17] Kurtyka P., Rylko N., Quantitative analysis of the particles distributions in reinforced composites, Composite Structures 2017, 182, 412-419.

[18] Krzaczek B., Rylko N., Kurtyka P., Effective conductivity of particle-reinforced composites with cracks at particle-

matrix interface, Composites Theory and Practice 2018, 18(2), 115-120.

[19] Agaliotis E., Rosenberger M., Ares A., Schvezov C., Influence of the shape of the particles in the solidification of composite materials, Procedia Materials Science 2012, December, 1, 58-63.

[20] Drygaś P., Gluzman S., Mityushev V., Nawalaniec W., Applied Analysis of Composite Media, Analytical and Computational Results for Materials Scientists and Engineers, Woodhead Publishing, 2019.

[21] Lakshmipathy J., Kulendran B., Reciprocating wear behaviour of 7075Al/SiC and 6061Al/Al_2O_3 composites: A study of effect of reinforcement, stroke and load, Tribology in Industry 2014, June, 36, 2, 117-126.

[22] Cerit A., Baki Karamis M., Nair F., Yildizli K., Effect of reinforcement particle size and volume fraction on wear behavior of metal matrix composites, Journal of the Balkan Tribological Association 2008, January 12, 4, 482-489.

[23] Deshmanya I.B., Purohit G., Development of mathematical model to predict micro-hardness of Al7075 and Al_2O_3 composites produced by stir-casting, Journal of Engineering Science and Technology Review 2012, March, 5, 1, 44-50.

[24] Pradhan S., Tapan G.S., Barman K., Sahoo P., Effect of SiC weight percentage on tribological properties of Al-SiC metal matrix composites under acid environment, Jurnal Tribologi 2017, June, 13, 21-35.

[25] Wieczorek J.M., Śledziona J., Dolata-Grosz J., Dyzia M.A., Zużycie i struktura powierzchni po współracy w warunkach tarcia technicznie suchego w kompozytach AK12 - cząstki ceramiczne, Kompozyty (Composites) 2003, 3, 6, 131-135.

[26] Dolata A.J., Dyzia M., Wieczorek J., Tribological properties of single (AlSi7/SiC_p, AlSi7/GC_{sf}) and hybrid (AlSi7/SiCp+ +GCsf) composite layers formed in sleeves via centrifugal casting, Materials 2019, 12(17), Article Number 2803; DOI: 10.3390/ma12172803.

[27] Chaubey A., Prashanth K.G., Wang Z., Scudino S., Mukhopadhyay N.K., Eckert J., Effect of particle size on microstructure and mechanical properties of al-based composite reinforced with 10 vol.% mechanically alloyed Mg-7.4% Al Particles, Technologies 2016, November, 4, 37, 1-8.

[28] Llorca J., An analysis of the influence of reinforcement fracture on the strength of discontinuously-reinforced metal-matrix composites, Acta Metallurgica et Materialia 1995, 43, 1, 181-192.

[29] Gan Y.X., Solomon D., Reinbolt M., Friction stir processing of particle reinforced composite materials, Materials 2010, January, 3, 1, 329-350.

[30] Balakrishnan M., Dinaharan I., Palanivel R., Sivaprakasam R., Synthesize of AZ31/TiC magnesium matrix composites using friction stir processing, Journal of Magnesium and Alloys 2015, January, 3, 1, 76-78.

[31] Azimi-Roeen G., Kashani-Bozorg S.F., Nosko M., Stefan N., Matko I., Formation of Al/($Al_{13}Fe_4$+Al_2O_3) nanocomposites via mechanical alloying and friction stir processing, Journal of Materials Engineering and Performance 2018, January, 27, 2, 471-482.

[32] Bauri R., Yadav D., Metal Matrix Composites by Friction Stir Processing, Elsevier, Woburn 2017.

[33] Jerome S., Govind Bhalchandra S., Kumaresh Babu S.,P, Ravisankar B., Influence of microstructure and experimental parameters on mechanical and wear properties of Al-TiC surface composite by FSP route, Journal of Minerals and Materials Characterization and Engineering 2012, 11, 5, 493-507.

[34] Wójcicka A., Mroczka K., Kurtyka P., Binkowski M., Wróbel Z., X-ray microtomography analysis of the aluminum alloy composite reinforced by SiC after friction stir processing, Journal of Materials Engineering and Performance 2014, June, 23, 9, 3215-3221.

[35] Abbasi M., Bagheri B., Dadaei M., Omidvar H., Rezaei M., The effect of FSP on mechanical, tribological, and corrosion behavior of composite layer developed on magnesium AZ91 alloy surface, The International Journal of Advanced Manufacturing Technology 2014, November, 77, 12, 2051-2058.

[36] Bozkurt Y., Uzun H.., Salman S., Microstructure and mechanical properties of friction stir welded particulate reinforced AA2124/SiC/25p-T4 composite, Journal of Composite Materials 2011, September, 45, 21, 2237-2245.

[37] Nallusamy D., Rajaram Narayanan M., An experimental analysis of aluminium alloy with tungsten carbide metal matrix composite through in-situ method using SEM, Rasayan Journal of Chemistry 2018, February, 11, 1, 355-360.

[38] Gluzman S., Mityushev V., Nawalaniec W., Computational Analysis of Structured Media, Academic Press, 2018.

[39] Molina P., Amalberto R., Rosso M., Mechanical characterization of aluminium alloys for high temperature applications part 2: Al-Cu, Al-Mg alloys, Metallurgical Science and Technology 2011, 29, 2, 5-13.

[40] Karthikeyan L., Senthilkumar V.S., Balasubramanian V., Natarajan S., Mechanical property and microstructural changes during friction stir processing of cast aluminum 2285 alloy, Materials and Design 2009, June, 30, 6, 2237-2242.

[41] Bousquet E., Quintin A.P., Puiggali M., Devos O., Touzet M., Relationship between microstructure, microhardness and corrosion sensitivity of an AA2024-T3 friction stir welded joint, Corrosion Science 2011, 53, 9, 3026-3034.

[42] Mishra R., Ma Z., Friction stir welding and processing, Materials Science and Engineering: R: Reports 2005, 50, 1, 1-78.

[43] Mroczka K., Dutkiewicz J., Lityńska-Dobrzyńska L., Pietras A., Microstructure and properties of fsw joints of 2017A/6013 aluminium alloys sheets, Archives of Materials Science and Engineering 2008, 33, 2, 93-96.

[44] Mroczka K., Dutkiewicz J., Pietras A., Microstructure of friction stir welded joints of 2017a aluminium alloy sheets, Journal of Microscopy 2010, March, 237, 3, 521-525.

[45] Kurtyka P., Effect of plastic deformation on the microstructure, size and distribution of SiC reinforcing particles in the cast F3K.10S composite, Rudy i Metale Nieżelazne Recykling 2015, 60, 7, 316-323.

[46] Hill R., Elastic properties of reinforced solids: Some theoretical principles, Journal of the Mechanics and Physics of Solids 1963, 11, 5, 357-372.

[47] Mityushev V., Representative cell in mechanics of composites and generalized Eisenstein-Rayleigh sums, Complex Variables and Elliptic Equations 2006, 51, 8-11, 1033-1045.

[48] Czapla R., Nawalaniec W., Mityushev V., Effective conductivity of random two-dimensional composites with circular non-overlapping inclusions, Computational Materials Science 2012, 63, 118-126.

[49] Nawalaniec W., Basic sums: A python package for computing structural sums and the effective conductivity of random composites, Journal of Open Source Software 2019, March, 4.

[50] Shafiei-Zarghani A., Kashani-Bozorg S., Zarei-Hanzaki A., Microstructures and mechanical properties of Al/Al_2O_3 surface nano-composite layer produced by friction stir processing, Materials Science and Engineering: A 2009, 500, 1, 84-91.

[51] Ma Z., Friction stir processing technology: A review, Metallurgical and Materials Transactions A 2008, 39, 3, 642-658.

[52] Rana H., Badheka V., Kumar A., Fabrication of Al7075/B4c surface composite by novel friction stir processing

(FSP) and investigation on wear properties, Procedia Technology 2016, February, 23, 519-528.
[53] Morisada Y., Fujii H., Nagaoka T., Fukusumi M., Effect of friction stir processing with SiC particles on microstructure and hardness of AZ31, Materials Science and Engineering: A 2006, 433, 1, 50-54.
[54] Ma Z., Sharma S., Mishra R., Effect of friction stir processing on the microstructure of cast A356 aluminum, Materials Science and Engineering: A 2006, 433, 1, 269-278.
[55] Olson E., Particle shape factors and their use in image analysis - Part 1: Theory, Journal of GXP Compliance 2011, 15, 3, 85-96.
[56] Guerra M., Schmidt C., McClure J., Murr L., Nunes A., Flow patterns during friction stir welding, Materials Characterization 2002, 49, 2, 95-101.
[57] Naeem H., Characterizations particulates of crushed particles (Al-Zn-Mg-Cu-Ni) for fabrication of surface composites al-alloy using friction stir processing, Muthanna Journal of Engineering and Technology (MJET) 2017, 56-65.
[58] Chen Y., Ni Q., Ke L., Interface characteristic of friction stir welding lap joints of Ti/Al dissimilar alloys, Transactions of Nonferrous Metals Society of China 2012, 22, 2, 299-304.
[59] Iwaszko J., Kudła K., Effect of friction stir processing (FSP) on microstructure and hardness of AlMg10/SiC composite, Bulletin of the Polish Academy of Sciences: Technical Sciences 2019, 67, 2, 185-182.
[60] Zheng F., Wu Y., Peng L., Li, X., Fu P., Ding W., Microstructures and mechanical properties of friction stir processed Mg-2.0Nd-0.3Zn-1.0Zr magnesium alloy, Journal of Magnesium and Alloys 2013, June, 1, 2, 122-127.
[61] Woo W., Balogh L., Ungar, T., Choo H., Feng Z., Grain structure and dislocation density measurements in a friction-stir welded aluminum alloy using X-ray peak profile analysis, Materials Science and Engineering: A 2008, 498, 1, 308-313.
[62] McNelley T., Swaminathan S., Su J., Recrystallization mechanisms during friction stir welding/processing of aluminum alloys, Scripta Materialia 2008, 58, 5, 349-354.

